

Image Forgery Localization with State Space Models

Zijie Lou and Gang Cao, *Member, IEEE*

Abstract—Pixel dependency modeling from tampered images is pivotal for image forgery localization. Current approaches predominantly rely on convolutional neural network (CNN) or Transformer-based models, which often either lack sufficient receptive fields or entail significant computational overheads. In this paper, we propose LoMa, a novel image forgery localization method that leverages the Selective State Space (S6) model for global pixel dependency modeling and inverted residual CNN for local pixel dependency modeling. Our method introduces the Mixed-SSM Block, which initially employs atrous selective scan to traverse the spatial domain and convert the tampered image into order patch sequences, and subsequently applies multi-directional S6 modeling. In addition, an auxiliary convolutional branch is introduced to enhance local feature extraction. This design facilitates the efficient extraction of global dependencies while upholding linear complexity. Upon modeling the pixel dependency with the SSM and CNN blocks, the pixel-wise forgery localization results are obtained by a simple MLP decoder. Extensive experimental results validate the superiority of LoMa over CNN-based and Transformer-based state-of-the-arts.

Index Terms—Image Forensics, Image Forgery Localization, State Space Models

I. INTRODUCTION

Image forgery localization (IFL), which aims to segment tampered regions in an image, is a fundamental yet challenging digital forensic task. Its utility spans many practical applications, including digital forensics, copyright protection and identity verification. IFL workflows typically encompass two primary stages: first, capturing the pixel dependency of the input tampered images, and secondly, leveraging this information to generate localization maps. Current methods for modeling pixel dependency predominantly rely on CNNs and Transformers-based models. However, as illustrated in the first three rows of Table I, these methods either (1) do not have sufficient receptive fields to capture inter-pixel correlations, or (2) suffer from prohibitive computational complexity.

On the other hand, Natural Language Processing (NLP) has recently seen the advent of structured state space models (SSMs). From a theoretical perspective, SSMs integrate the advantages of Recurrent Neural Networks (RNNs) with those of Convolutional Neural Networks (CNNs), capitalizing on the global receptive field characteristics of RNNs while also

TABLE I
COMPARISON OF THE MODEL DESIGN FOR PIXEL DEPENDENCY MODELING OF LOMA AND EXISTING METHODS. LOMA ENJOYS BOTH THE ADVANTAGES OF A LARGE RECEPTIVE FIELD AND LINEAR COMPLEXITY.

Architecture	Linear Complexity	Global Receptive Field	Representative Method
CNN	✓	✗	CAT-Net [1]
Transformer	✗	✓	TruFor [2]
Mamba	✓	✓	LoMa (Ours)

benefiting from the computational efficiency of CNNs. A particularly noteworthy SSM is the Selective State Space Model (S6), commonly referred to as Mamba, which has attracted considerable interest within the vision research community. The innovative aspect of Mamba lies in its ability to render SSM parameters time-variant (i.e., dependent on the data), allowing it to effectively identify pertinent contexts within sequences—a critical factor for improving model performance. Nevertheless, to the best of our knowledge, **S6 has not yet been applied to image forgery localization task.**

In this paper, we propose LoMa, a novel image forgery localization method that adapts the S6 model for efficient global pixel dependency modeling. As shown in Table I, LoMa provides the advantages of a global receptive field with linear complexity. Specifically, our method introduces the Mixed-SSM Block, which initially utilizes atrous selective scanning to navigate the spatial domain and convert the tampered image into ordered patch sequences, followed by the implementation of multi-directional S6 modeling. Moreover, an auxiliary convolutional branch is integrated to enhance the extraction of local features. After modeling the pixel dependencies with the SSM and CNN blocks, pixel-wise forgery localization results are achieved using a simple MLP decoder. Extensive experimental results substantiate the superiority of our approach, LoMa, over existing state-of-the-art methods based on CNNs and Transformers.

The rest of this letter is organized as follows. The proposed LoMa scheme is described in Section II, followed by extensive experiments and discussions in Section III. We draw the conclusions in Section IV.

II. PROPOSED LOMA SCHEME

A. Preliminaries

State Space Models (SSMs) are primarily motivated by continuous linear time-invariant (LTI) systems, which utilize an implicit latent state $h(t) \in \mathbb{R}^N$ to map a scalar input

Zijie Lou and Gang Cao are with the School of Computer and Cyber Sciences, Communication University of China, Beijing 100024, China, and also with the State Key Laboratory of Media Convergence and Communication, Communication University of China, Beijing 100024, China (e-mail: {louzijie2022, gangcao}@cuc.edu.cn).

Code and dataset are available at <https://github.com/multimediaFor/LoMa>.

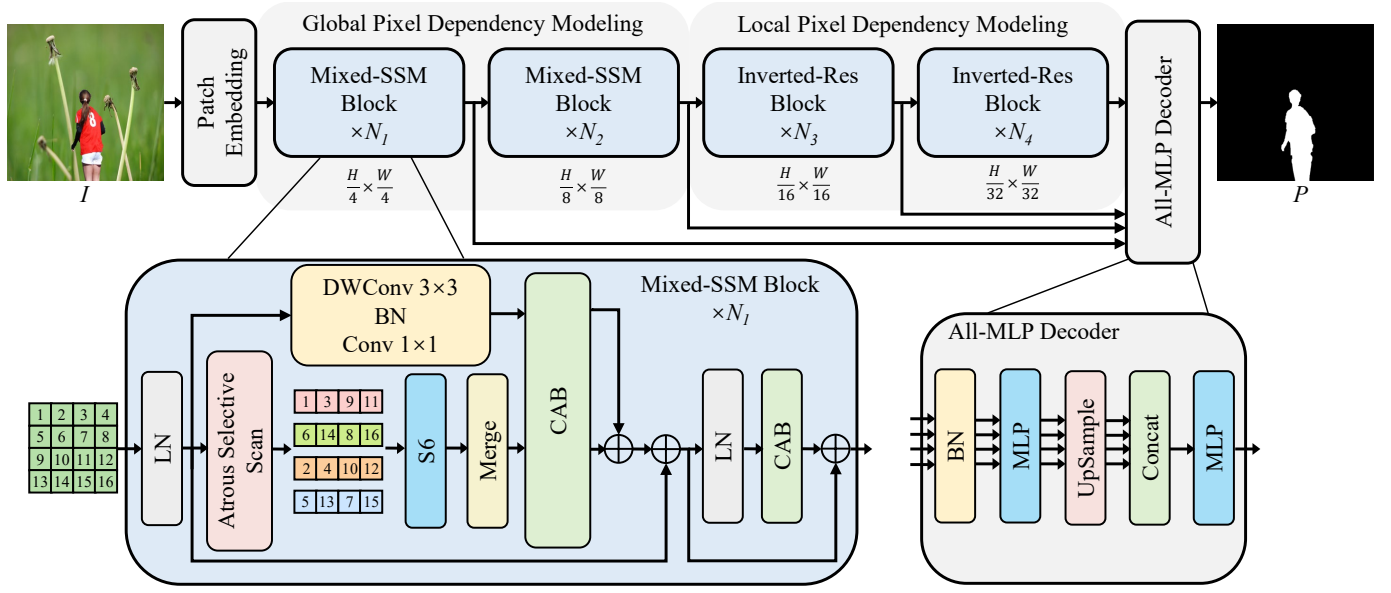


Fig. 1. Proposed image forgery localization scheme LoMa. $N_i = \{4, 4, 15, 4\}$, LN, BN, and CAB refer to Layer Normalization, Batch Normalization, and Channel Attention Block, respectively.

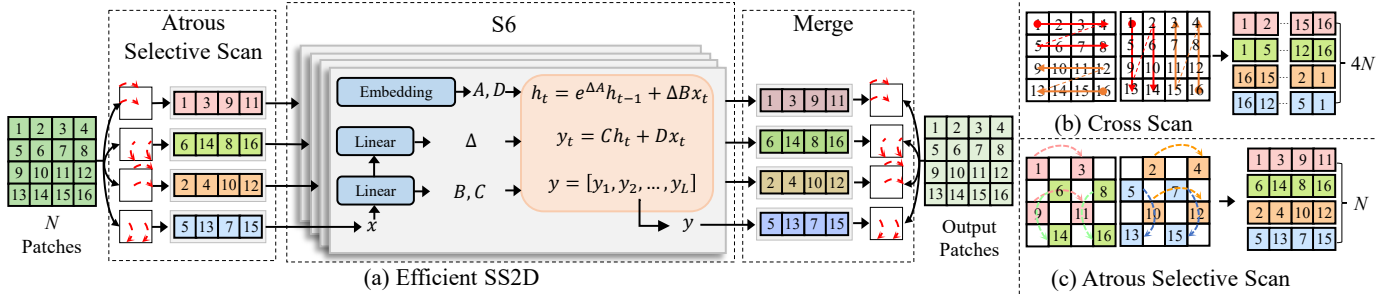


Fig. 2. Efficient SS2D.

sequence or function $x(t) \in \mathbb{R}$ to a scalar output $y(t) \in \mathbb{R}$. In particular, SSMs can be formulated as an ordinary differential equation (ODE):

$$h'(t) = Ah(t) + Bx(t) \quad (1)$$

$$y(t) = Ch(t) \quad (2)$$

where contains evolution matrix $A \in \mathbb{R}^{N \times N}$, projection parameters $B \in \mathbb{R}^{N \times 1}$ and $C \in \mathbb{R}^{1 \times N}$. However, solving the above differential equation directly in deep learning settings is challenging, and thus requires approximation through discretization. Recent works on state space models (SSMs) [3] propose the introduction of a timescale parameter Δ to transform the continuous matrices A and B into their discrete counterparts \bar{A} and \bar{B} , i.e.,

$$h_t = \bar{A}h_{t-1} + \bar{B}x_t \quad (3)$$

$$y_t = Ch_t, \quad (4)$$

$$\bar{A} = \exp(\Delta A) \quad (5)$$

$$\bar{B} = (\Delta A)^{-1} (\exp(\Delta A) - I) \cdot \Delta B \quad (6)$$

The above SSMs are applied independently to each channel, with data-independent parameters, meaning that \bar{A} , \bar{B} , and C

remain constant for any input within the same channel. This characteristic limits their flexibility in modeling sequences. To address this, Mamba [4] introduces selective SSMs (S6), which dynamically generate the parameters for each input data $x_i \in \mathbb{R}^L$ based on the entire input sequence x_i :

$$B_i = S_B x_i \quad (7)$$

$$C_i = S_C x_i \quad (8)$$

$$\Delta_i = \text{softplus}(S_\Delta x_i) \quad (9)$$

where $S_B \in \mathbb{R}^{N \times L}$, $S_C \in \mathbb{R}^{N \times L}$, $S_\Delta \in \mathbb{R}^{L \times L}$ are linear projection layers. The B_i and C_i are shared for all channels of x_i , Δ_i contains Δ of L channels, and A are the same as previous SSMs. By the discretization in equations 5 and 6, \bar{A} and \bar{B} become different based on input data.

B. Overall pipeline

Given one tampered image $I \in \mathbb{R}^{H \times W \times 3}$, the objective of the image forgery localization task is to generate the localization map $P \in \mathbb{R}^{H \times W \times 1}$. As illustrated in Fig. 1, the overall pipeline of LoMa consists of three main components: global pixel dependency modeling, local pixel dependency

TABLE II
TRAINING / TESTING SPLIT AND CHARACTERISTIC OF PUBLIC
BENCHMARK DATASETS.

Dataset	Type	Training	Testing
SP-COCO [1]	Splicing	200k	-
CM-COCO [1]	Copy-move	200k	-
CM-RAISE [1]	Copy-move	200k	-
CM-C-RAISE [1]	Copy-move	200k	-
CASIAv2 [11]	Splicing, Copy-move	5123	-
IMD [12]	Splicing, Copy-move, Removal	2010	-
Columbia [13]	Splicing	-	160
CASIAv1 [11]	Splicing, Copy-move	-	920
NIST [14]	Splicing, Copy-move, Removal	-	564
Coverage [15]	Copy-move	-	100
Wild [16]	Splicing	-	201
MISD [17]	Splicing	-	227

modeling, and feature decoding. Firstly, the image is divided into patches to obtain \hat{I} . Then, we employ a set of mixed-ssm blocks to extract global features from \hat{I} , progressively reducing the resolution to facilitate more efficient global pixel dependency modeling. This process can be formulated as:

$$X_1, X_2 = \text{Mixed-SSM Blocks}(\hat{I}) \quad (10)$$

where $X_1 \in \mathbb{R}^{\frac{H}{4} \times \frac{W}{4} \times C_1}$ and $X_2 \in \mathbb{R}^{\frac{H}{8} \times \frac{W}{8} \times C_2}$. Next, we perform local pixel dependency modeling using inverted residual blocks [5]:

$$X_3, X_4 = \text{Inverted-Res Blocks}(X_2) \quad (11)$$

where $X_3 \in \mathbb{R}^{\frac{H}{16} \times \frac{W}{16} \times C_3}$ and $X_4 \in \mathbb{R}^{\frac{H}{32} \times \frac{W}{32} \times C_4}$. Such allocation of SSM and CNN blocks is aimed at promoting SSMs in the early stages with high resolutions for better global capture, while adopting CNNs at low resolutions for improved efficiency.

Finally, the pixel-wise forgery localization map P is obtained by a simple MLP decoder [6]:

$$P = \text{ALL-MLP Decoder}(X_1, X_2, X_3, X_4) \quad (12)$$

C. Efficient SS2D

In terms of visual tasks, VMamba [7] proposed the 2D Selective Scan (SS2D), which maintains the integrity of 2D image structures by scanning four directed feature sequences. Each sequence is processed independently within an S6 block and then being combined to form a comprehensive 2D feature map. In this paper, an efficient atrous selective scan [8] is used. As shown in Fig. 2, Given a feature map with N patches, instead of cross-scan whole patches, we skip scan patches with a step size p and partition into selected spatial dimensional features. Such efficient scan approach reduces computational demands ($4N \rightarrow N$) while preserving global feature maps. Drawing inspiration from [9], who identified the lack of locality and inter-channel interaction in SSMs, we replace the multilayer perceptron (MLP) with a Channel-Attention Block (CAB) [10].

III. EXPERIMENTS

A. Experimental Settings

1) *Datasets*: As shown in Table II, our model is trained using the same datasets with CAT-Net [1] and TruFor [2], and tested on other six public available datasets, including Columbia [13], CASIAv1 [11], NIST [14], Coverage [15], Wild [16], and MISD [17].

2) *Compared Methods*: To validate the effectiveness of state space models, we selected six representative image forgery detection methods from the most advanced CNN-based and Transformer-based approaches over the past three years for comparison. The CNN-based methods include PSCC [18], MVSS++ [19], and CAT-Net [1], while the Transformer-based methods include EITLNet [20], ProFact [21], and TruFor [2].

3) *Evaluation metrics*: Similar to previous works [2], [22], [23], the accuracy of pixel-level forgery localization is measured by F1 and IoU. The fixed threshold 0.5 is adopted to binarize the localization probability map. Considering the obvious imbalance of image sample numbers across different datasets, Considering the evident imbalance in the number of image samples across different datasets, we follow the approach outlined in [24] to calculate the average F1 and IoU.

4) *Implementation details*: The proposed LoMa is implemented by PyTorch. We train the network on a single A100 40G GPU. The learning rate starts from 1e-4 and decreases by the plateau strategy. Adam is adopted as the optimizer, batch size is 8 and all the images used in training are resized to 512×512 pixels. The common data augmentations, including flipping, blurring, compression and noising are adopted. The related parameters are set empirically as $\alpha = 0.5$ and $\gamma = 2$.

5) *Loss function*: LoMa is trained using Focal loss [25]:

$$\begin{aligned} \mathcal{L}_{\text{Focal}} = & - \sum_{i,j} \alpha (1 - \mathbf{P}_{ij})^\gamma * \mathbf{G}_{ij} \log(\mathbf{P}_{ij}) \\ & - \sum_{i,j} (1 - \alpha) \mathbf{P}_{ij}^\gamma * (1 - \mathbf{G}_{ij}) \log(1 - \mathbf{P}_{ij}) \end{aligned} \quad (13)$$

where $\mathbf{G}_{ij} \in \{0, 1\}$ denotes the pixel-level label and $\mathbf{P}_{ij} \in (0, 1)$ denotes the corresponding prediction result. α is the weight parameter to balance inpainted and authentic pixels and γ is the parameter for hard mining.

B. Comparison With State-of-the-art Methods

LoMa is compared with six state-of-the-art methods, i.e., PSCC [18], MVSS++ [19], and CAT-Net [1], EITLNet [20], ProFact [21], and TruFor [2].

Table III reports the compared results on six publicly available datasets. Table III shows that LoMa achieves the best or second-best performance on almost every testing dataset, with the highest average localization accuracy across six testing datasets. For instance, LoMa achieved the highest localization accuracy on the Columbia and CASIAv1 datasets, while obtaining second-best performance on the NIST, Coverage, and MISD datasets. Overall, compared to CNN-based and Transformer-based methods, the Mamba-based LoMa demonstrates superior performance in image forgery localization task.

TABLE III

IMAGE FORGERY LOCALIZATION PERFORMANCE F1[%] AND IOU[%]. THE BEST RESULTS ARE HIGHLIGHTED IN RED AND THE SECOND-BEST RESULTS ARE HIGHLIGHTED IN BLUE.

Method	Architecture	Columbia		CASIAv1		NIST		Coverage		Wild		MISD		Average	
		F1	IoU	F1	IoU	F1	IoU	F1	IoU	F1	IoU	F1	IoU	F1	IoU
PSCC [18]	CNN	61.5	48.3	46.3	41.0	18.7	13.5	44.4	33.6	10.8	8.1	65.6	52.4	38.9	32.2
MVSS++ [19]	CNN	68.4	59.6	45.1	39.7	29.4	24.0	44.5	37.9	29.5	21.9	65.9	52.4	43.4	36.7
CAT-Net [1]	CNN	79.3	74.6	71.0	63.7	30.2	23.5	28.9	23.0	34.1	28.9	39.4	31.3	52.4	45.6
EITLNet [20]	Transformer	87.6	84.2	55.7	52.0	33.0	26.7	44.3	35.3	51.9	43.0	75.5	63.8	53.3	47.4
ProFact [21]	Transformer	84.5	82.7	56.4	50.2	43.1	36.2	51.1	43.1	64.5	56.1	63.6	50.1	56.3	49.2
TruFor [2]	Transformer	79.8	74.0	69.6	63.2	47.2	39.6	52.3	45.0	61.2	51.9	60.0	47.5	62.0	54.3
LoMa (Ours)	Mamba	86.8	85.5	73.2	68.1	43.1	37.2	48.9	43.1	48.6	41.4	68.7	56.2	62.5	56.5

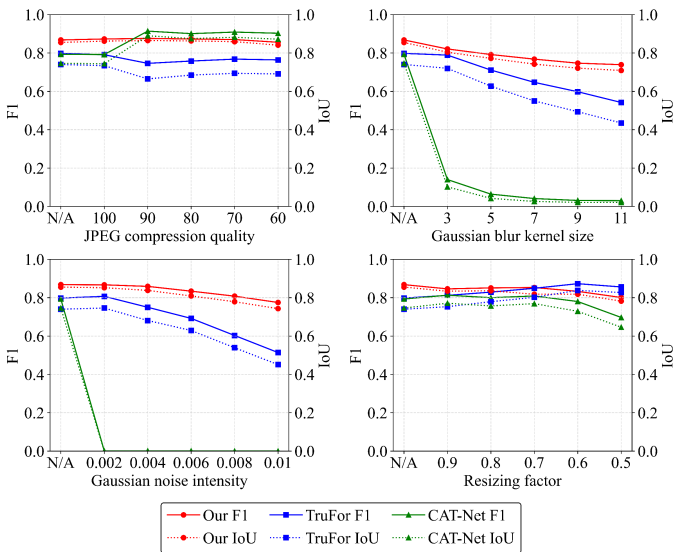


Fig. 3. Robustness against different post-processing manipulations on the Columbia dataset.

C. Robustness Evaluation

We first assess the robustness of image forgery localization methods against the complex post operations introduced by online social networks (OSNs). Following the prior work [23], the four forgery datasets transmitted through Facebook, Weibo, Wechat and Whatsapp platforms are tested. Table IV shows that, our method mostly achieves the highest accuracy across the four datasets for each social network platform. Among the compared methods, LoMa enjoys the smallest performance loss incurred by OSNs. Note that CAT-Net achieves higher performance on the processed Columbia dataset due to its specialized learning of JPEG compression artifacts. However, it shows obvious performance decline on other datasets, for instance, with F1=91.8% on the Facebook version of Columbia while with F1=13.9% on the Wechat version of CASIAv1. In contrast, our LoMa consistently keeps high localization accuracy across all OSN transmissions. Such results verify the robustness of LoMa against the online social networks.

Following the prior works [18], [19], the robustness against post JPEG compression, Gaussian blur, Gaussian noise and resizing is also evaluated on the Columbia dataset. The results

TABLE IV

ROBUSTNESS PERFORMANCE F1[%] AND IOU[%] AGAINST ONLINE SOCIAL NETWORKS (OSNs) POST-PROCESSING, INCLUDING FACEBOOK (FB), WECHAT (WC), WEIBO (WB) AND WHATSAPP (WA). THE BEST RESULTS ARE HIGHLIGHTED IN RED.

Method	OSNs	CASIAv1		Columbia		NIST	
		F1	IoU	F1	IoU	F1	IoU
CAT-Net [1]	FB	63.3	55.9	91.8	90.0	15.1	11.9
TruFor [2]		67.2	60.5	74.9	67.1	35.3	27.8
LoMa (Ours)		70.3	64.8	87.2	86.2	41.9	36.1
CAT-Net [1]	WC	13.9	10.6	84.8	80.8	19.1	14.9
TruFor [2]		56.9	50.8	77.3	70.3	35.1	27.4
LoMa (Ours)		58.3	52.7	87.2	86.0	39.9	34.2
CAT-Net [1]	WB	42.5	36.2	92.1	89.7	20.8	16.0
TruFor [2]		63.7	57.6	80.0	73.1	33.2	26.2
LoMa (Ours)		69.9	65.0	86.5	85.3	40.9	35.5
CAT-Net [1]	WA	42.3	37.8	92.1	89.9	20.1	16.8
TruFor [2]		66.3	59.9	74.7	66.7	32.3	25.6
LoMa (Ours)		69.8	64.4	87.2	86.1	40.7	35.2

shown in Fig. 3 verify the high robustness of our LoMa against such post-processing. LoMa performs the best in all cases. Specially, the blur and noise manipulations greatly reduce the performance of CAT-Net and TruFor, but have minimal impact on our method. Take the noise for example, although F1 values of CAT-Net and TruFor decrease from 0.8 to 0 and 0.5, respectively, that of LoMa always keeps above 0.75 across different noise intensities.

IV. CONCLUSION

In this paper, we propose LoMa, the first image forgery localization method based on state space models. LoMa employs a selective state space model to capture global pixel dependencies. Compared to CNN-based methods, LoMa has a global receptive field, and compared to Transformer-based methods, LoMa exhibits linear computational complexity. Extensive evaluation results have verified the effectiveness of our proposed image forgery localization scheme and demonstrated the great potential of state space models in forensic tasks. In the future, we will explore more efficient applications of state space models in the field of digital forensics.

REFERENCES

- [1] M.-J. Kwon, S.-H. Nam, I.-J. Yu, H.-K. Lee, and C. Kim, "Learning jpeg compression artifacts for image manipulation detection and localization," *International Journal of Computer Vision*, vol. 130, no. 8, pp. 1875–1895, 2022.
- [2] F. Guillaro, D. Cozzolino, A. Sud, N. Dufour, and L. Verdoliva, "Trufor: Leveraging all-round clues for trustworthy image forgery detection and localization," in *Proceedings of the IEEE/CVF Conference on Computer Vision and Pattern Recognition*, 2023, pp. 20 606–20 615.
- [3] A. Gu, K. Goel, and C. Ré, "Efficiently modeling long sequences with structured state spaces," in *Proceedings of the International Conference on Learning Representations*, 2021.
- [4] A. Gu and T. Dao, "Mamba: Linear-time sequence modeling with selective state spaces," *arXiv preprint arXiv:2312.00752*, 2023.
- [5] M. Sandler, A. Howard, M. Zhu, A. Zhmoginov, and L.-C. Chen, "Mobilenetv2: Inverted residuals and linear bottlenecks," in *Proceedings of the IEEE/CVF Conference on Computer Vision and Pattern Recognition*, 2018, pp. 4510–4520.
- [6] E. Xie, W. Wang, Z. Yu, A. Anandkumar, J. M. Alvarez, and P. Luo, "Segformer: Simple and efficient design for semantic segmentation with transformers," *Advances in Neural Information Processing Systems*, vol. 34, pp. 12 077–12 090, 2021.
- [7] Y. Liu, Y. Tian, Y. Zhao, H. Yu, L. Xie, Y. Wang, Q. Ye, and Y. Liu, "Vmamba: Visual state space model," *arXiv preprint arXiv:2401.10166*, 2024.
- [8] X. Pei, T. Huang, and C. Xu, "Efficientvmamba: Atrous selective scan for light weight visual mamba," *arXiv preprint arXiv:2403.09977*, 2024.
- [9] H. Guo, J. Li, T. Dai, Z. Ouyang, X. Ren, and S.-T. Xia, "Mambair: A simple baseline for image restoration with state-space model," in *Proceedings of the Conference on European Conference on Computer Vision*, 2025, pp. 222–241.
- [10] J. Hu, L. Shen, and G. Sun, "Squeeze-and-excitation networks," in *Proceedings of the IEEE/CVF Conference on Computer Vision and Pattern Recognition*, 2018, pp. 7132–7141.
- [11] J. Dong, W. Wang, and T. Tan, "Casia image tampering detection evaluation database," in *Proceedings of the IEEE China Summit and International Conference on Signal and Information Processing*, 2013, pp. 422–426.
- [12] A. Novozamsky, B. Mahdian, and S. Saic, "Imd2020: a large-scale annotated dataset tailored for detecting manipulated images," in *Proceedings of the IEEE/CVF Winter Conference on Applications of Computer Vision Workshops*, 2020, pp. 71–80.
- [13] J. Hsu and S. Chang, "Columbia uncompressed image splicing detection evaluation dataset," *Columbia DVMM Research Lab*, 2006.
- [14] H. Guan, M. Kozak, E. Robertson, Y. Lee, A. N. Yates, A. Delgado, D. Zhou, T. Kheyrkhan, J. Smith, and J. Fiscus, "Mfc datasets: Large-scale benchmark datasets for media forensic challenge evaluation," in *Proceedings of the IEEE Winter Applications of Computer Vision Workshops*, 2019, pp. 63–72.
- [15] B. Wen, Y. Zhu, R. Subramanian, T.-T. Ng, X. Shen, and S. Winkler, "Coverage—a novel database for copy-move forgery detection," in *Proceedings of the IEEE International Conference on Image Processing*, 2016, pp. 161–165.
- [16] M. Huh, A. Liu, A. Owens, and A. A. Efros, "Fighting fake news: Image splice detection via learned self-consistency," in *Proceedings of the European Conference on Computer Vision*, 2018, pp. 101–117.
- [17] K. D. Kadam, S. Ahirrao, and K. Kotecha, "Multiple image splicing dataset (misd): a dataset for multiple splicing," *Data*, vol. 6, no. 10, p. 102, 2021.
- [18] X. Liu, Y. Liu, J. Chen, and X. Liu, "Pssc-net: Progressive spatio-channel correlation network for image manipulation detection and localization," *IEEE Transactions on Circuits and Systems for Video Technology*, vol. 32, no. 11, pp. 7505–7517, 2022.
- [19] C. Dong, X. Chen, R. Hu, J. Cao, and X. Li, "Mvss-net: Multi-view multi-scale supervised networks for image manipulation detection," *IEEE Transactions on Pattern Analysis and Machine Intelligence*, vol. 45, no. 3, pp. 3539–3553, 2022.
- [20] K. Guo, H. Zhu, and G. Cao, "Effective image tampering localization via enhanced transformer and co-attention fusion," in *Proceedings of the IEEE International Conference on Acoustics, Speech and Signal Processing*, 2024, pp. 4895–4899.
- [21] H. Zhu, G. Cao, and X. Huang, "Progressive feedback-enhanced transformer for image forgery localization," *arXiv preprint arXiv:2311.08910*, 2023.
- [22] C. Kong, A. Luo, S. Wang, H. Li, A. Rocha, and A. C. Kot, "Pixel-inconsistency modeling for image manipulation localization," *arXiv preprint arXiv:2310.00234*, 2023.
- [23] H. Wu, J. Zhou, J. Tian, J. Liu, and Y. Qiao, "Robust image forgery detection against transmission over online social networks," *IEEE Transactions on Information Forensics and Security*, vol. 17, pp. 443–456, 2022.
- [24] Z. Lou, G. Cao, K. Guo, H. Zhu, and L. Yu, "Exploring multi-view pixel contrast for general and robust image forgery localization," *arXiv preprint arXiv:2406.13565*, 2024.
- [25] T.-Y. Lin, P. Goyal, R. Girshick, K. He, and P. Dollár, "Focal loss for dense object detection," in *Proceedings of the IEEE/CVF International Conference on Computer Vision*, 2017, pp. 2980–2988.